Nanoelectronics and Its New Materials – A NEW ERA OF NANOSCIENCE

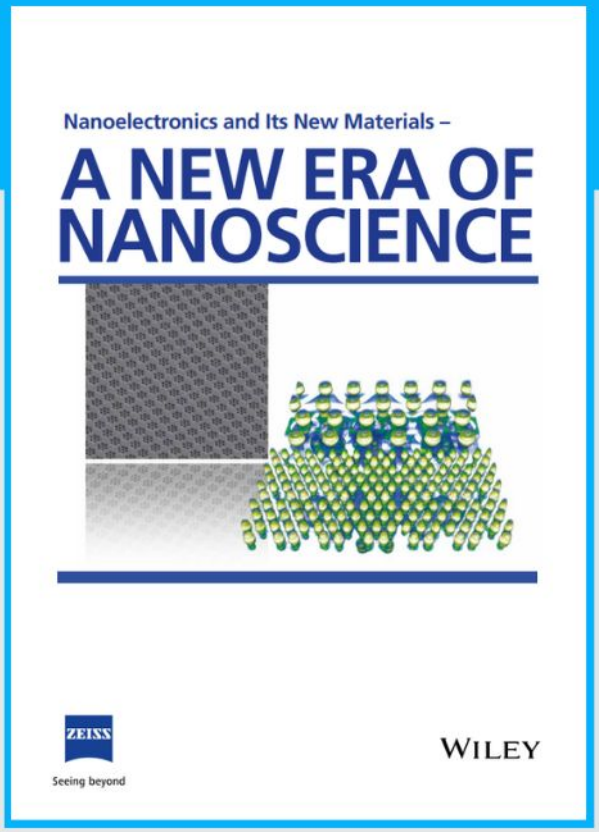

Discover the recent advances in electronics research and fundamental nanoscience.

Nanotechnology has become the driving force behind breakthroughs in engineering, materials science, physics, chemistry, and biological sciences. In this compendium, we delve into a wide range of novel applications that highlight recent advances in electronics research and fundamental nanoscience. From surface analysis and defect detection to tailored optical functionality and transparent nanowire electrodes, this eBook covers key topics that will revolutionize the future of electronics.

To get your hands on this valuable resource and unleash the power of nanotechnology, simply download the eBook now. Stay ahead of the curve and embrace the future of electronics with nanoscience as your guide.

ZEISS

Seeing beyond

WILEY

NANO · MICRO small
www.small-journal.com

Cell-Like Capsules with "Smart" Compartments

*So Hyun Ahn, Leah K. Borden, William E. Bentley, and Srinivasa R. Raghavan**

Eukaryotic cells have inner compartments (organelles), each with distinct properties and functions. One mimic of this architecture, based on biopolymers, is the multicompartment capsule (MCC). Here, MCCs in which the inner compartments are *chemically unique* and "*smart*," i.e., responsive to distinct stimuli in an *orthogonal* manner are created. Specifically, one compartment alone is induced to degrade when the MCC is contacted with an enzyme while other compartments remain unaffected. Similarly, just one compartment gets degraded upon contact with reactive oxygen species generated from hydrogen peroxide (H_2O_2). And thirdly, one compartment alone is degraded by an external, physical stimulus, namely, by irradiating the MCC with ultraviolet (UV) light. All these specific responses are achieved without resorting to complicated chemistry to create the compartments: the multivalent cation used to crosslink the biopolymer alginate (Alg) is simply altered. Compartments of Alg crosslinked by Ca^{2+} are shown to be sensitive to enzymes (alginate lyases) but not to H_2O_2 or UV, whereas the reverse is the case with Alg/Fe^{3+} compartments. These results imply the ability to selectively burst open a compartment in an MCC "on-demand" (i.e., as and when needed) and using biologically relevant stimuli. The results are then extended to a sequential degradation, where compartments in an MCC are degraded one after another, leaving behind an empty MCC lumen. Collectively, this work advances the MCC as a platform that not only emulates key features of cellular architecture, but can also begin to capture rudimentary cell-like behaviors.

1. Introduction

The focus of this paper is on multicompartment capsules (MCCs), which are a class of biopolymer-based container structures with smaller capsules (compartments) in them.[1–5] The inspiration for making MCCs comes from the architecture of a eukaryotic cell, which has organelles like mitochondria, lysosomes, and peroxisomes in it.[6–9] Each type of organelle has distinct contents and membrane, which together dictate its unique function within a cell.[8,9] For example, lysosomes have an *acidic* environment in them that facilitates degradation of proteins.[6] Peroxisomes create an *oxidative* environment within them, which facilitates the metabolism of lipids.[6,10] Another class of organelles present in plant cells are the chloroplasts, which are involved in capturing energy from sunlight. An important point to note here is that the organelles are chemically "*orthogonal*" to one another. For instance, the response to sunlight is unique to chloroplasts while degradation under acidic conditions is exclusive to lysosomes.

Some of the challenges in designing MCCs (or more broadly, any kind of "artificial cell" or "protocell") are: a) to make these with a prescribed number of compartments; b) to make each compartment distinct in terms of its contents; and c) to achieve unique responses or functions for each compartment.[8,9] The synthesis of MCCs should also ideally be simple, quick, and versatile. All these considerations have guided our approach.[11,12] We have made MCCs using alginate (Alg), an anionic biopolymer that is widely used in biological applications due to its availability, low cost, and ability to form gels/capsules under mild conditions. We developed a water–air microfluidic device to create microscale MCCs,[11] and this ensured that all compartments had an aqueous interior with ambient pH and ionic strength. Using this approach, we were able to address the first two challenges listed above. For example, we reported MCCs with two compartments, each containing a different type of enzyme or nanoparticle.[11] Compared to MCCs prepared from lipids,[13] block copolymers,[1,4] proteins,[14] or multiple emulsions,[15] our Alg-based MCCs are far easier to create. No complex polymers or lipids need to be synthesized, nor is there a need for expensive or time-consuming fabrication techniques.

In this study, we enhance the sophistication of our Alg-based MCCs by making the inner compartments "*smart*," i.e., responsive to various stimuli (**Figure 1**). Thereby, we address the third challenge above, which is to make the compartments respond distinctly. For this, we endow each compartment with a *unique chemical signature* by simply using different multivalent cations to crosslink Alg (among Ca^{2+}, Fe^{3+}, Cu^{2+}, etc.) for each compartment. As an example of the final construct, Figure 1 shows an MCC with two compartments. One compartment (C1) alone gets degraded by enzymes from the alginate lyase family. A

S. H. Ahn, W. E. Bentley, S. R. Raghavan
Department of Chemical and Biomolecular Engineering
University of Maryland
College Park, MD 20742, USA
E-mail: sraghava@umd.edu

L. K. Borden, W. E. Bentley, S. R. Raghavan
Fischell Department of Bioengineering
University of Maryland
College Park, MD 20742, USA

The ORCID identification number(s) for the author(s) of this article can be found under https://doi.org/10.1002/smll.202206693.

DOI: 10.1002/smll.202206693

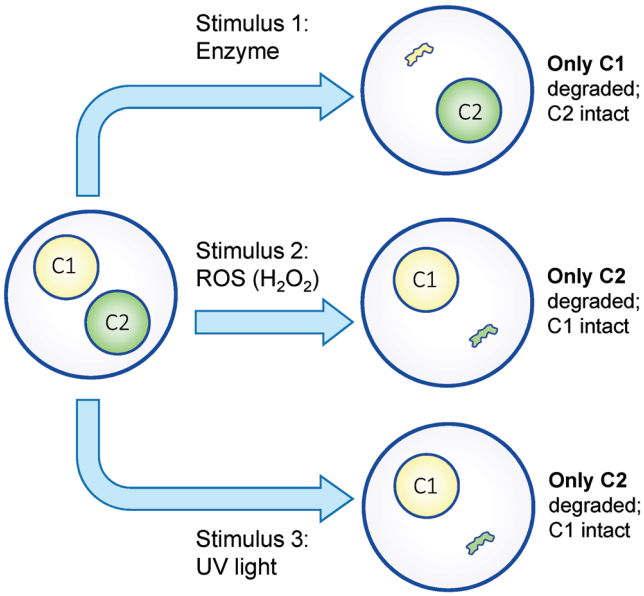

Figure 1. Schematic overview of this study on multicompartment capsules (MCCs) conceptually illustrating the "smart" response of the inner compartments. When exposed to different chemical or physical stimuli, a specific compartment of the MCC is degraded.

second compartment (C2) is selectively degraded by reactive oxygen species (ROS) formed from hydrogen peroxide (H_2O_2). Lastly, C2 alone is also degraded by exposure to ultraviolet (UV) light. The schematics illustrate the *orthogonal* responses of the compartments to the stimuli. That is, a given stimulus affects only one compartment while the other remains unaffected. Such specificity is enabled through the cation selected: for example, enzymes degrade Alg/Ca^{2+} compartments, but not Alg/Fe^{3+} ones, while the reverse is true with ROS. Note that the stimuli of interest here include chemical cues (ROS), biochemical cues (enzymes), and physical cues (UV light). All these stimuli have biological relevance and are distinct from the more common stimuli usually studied in relation to protocells, namely, temperature and pH.[12,15] At the end of the paper, we will also demonstrate the sequential destruction of two compartments in an MCC that relies on the successive application of two different stimuli.

2. Results and Discussion

We synthesized our Alg-based MCCs as follows. First, we prepared the inner compartments by dropping a 2% Alg solution into 0.1 M Ca^{2+} (or other cations like Fe^{3+}) using a needle and incubating for 1 h (see the Experimental Section for details). In the process, the Alg chains in the droplet became crosslinked by the multivalent cations. The resulting compartments (≈500 µm each) were then resuspended in a 2% Alg solution and dropped into 0.1 M Ca^{2+} to form the MCC (~5 mm diameter).[11,12] Figure S1 (Supporting Information) shows a schematic of this MCC synthesis. We typically created MCCs with two inner compartments (C1 and C2) where each compartment was responsive to an orthogonal stimulus. (If more compartments were present, the images looked confusing and are hence avoided for the sake of clarity.) Note that we refer to the compartments as capsules (rather than gels or beads) because the ionic crosslinking is not always uniform—i.e., the outer zones are typically crosslinked more than the inner core, giving the capsules a core–shell structure.[11] This is consistent with the nomenclature from our earlier papers.[11,12]

2.1. Degradation of a Compartment by an Enzyme

Alg capsules can be degraded by enzymes from the alginate lyase (Alg-lyase) family.[16–19] The enzyme catalyzes the cleavage of Alg chains by β-elimination, where the 4-O-glycosidic bonds between monomers are broken (see arrows in **Figure 2**A).[16] Long Alg chains are thus cleaved into oligomers. The activity of Alg-lyase depends on pH, temperature, and the nature of the cation used to crosslink Alg.[16–19] We exploit the fact that Alg-lyase degrades Alg/Ca^{2+} capsules but not Alg/Fe^{3+} capsules (because Fe^{3+} inhibits the enzyme while Ca^{2+} does not).[18] This is first shown in Figure 2A with a mixture of these capsules in a Petri dish. To distinguish the two sets of capsules, we embedded trace amounts (~0.01%) of carbon black nanoparticles (CB-NPs) in the Alg/Ca^{2+} capsules and iron-oxide nanoparticles (IO-NPs) in the Alg/Fe^{3+} capsules—thus, the two have a gray and an orange color, respectively (Image A1 in Figure 2A). In the presence of 1 unit mL^{-1} of the enzyme, all the Alg/Ca^{2+} capsules degrade completely over the course of 60 min at 37 °C. Thus, the only capsules remaining in the Petri dish (Image A2 in Figure 2A) are the Alg/Fe^{3+} ones.

The above result was obtained under two scenarios: a) if the enzyme was added to the solution around the capsules or b) if the enzyme was encapsulated in one or both capsules.[16,20] Note that enzyme molecules as well as nanoparticles remain sequestered in the capsules—i.e., they do not leak out unless the capsule is degraded.[20] The reason is that the Alg network has a mesh or pore size around 5 nm, which is smaller than the typical sizes of enzymes (~5–10 nm).[20,21] In our preferred experimental mode, we made Alg/Ca^{2+} capsules with encapsulated enzyme and monitored the time it takes for these capsules to self-degrade. This time is inversely proportional to the concentration of the enzyme (Figure 2B), consistent with previous studies.[16,20] A linear decrease in this time (measured up to the point when the capsules are completely degraded) is shown by the data: from ≈180 min for 0.1 units mL^{-1} of enzyme to ≈60 min for 1 unit mL^{-1}.

Next, we translate the enzymatic selectivity to an MCC (Figure 2C). The figure shows an MCC containing both an Alg/Ca^{2+} compartment (red) with 1 unit mL^{-1} of Alg-lyase in it as well as an Alg/Fe^{3+} compartment (light-orange). The colors are due to IO-NPs embedded in the compartments at different concentrations. At $t = 0$, the MCC is placed in phosphate buffered saline (PBS) (pH 7.4) at 37 °C (Image C1). Within 30 min, the IO-NPs are seen to leak out of the Alg/Ca^{2+} compartment into the solution, which is a sign that the compartment is getting degraded (Image C2). After 60 min, the degradation of the Alg/Ca^{2+} compartment is complete (Image C3), whereas the Alg/Fe^{3+} one remains intact. Thus, we have successfully demonstrated an MCC in which one compartment selectively responds to a stimulus. As a further point of interest, we have

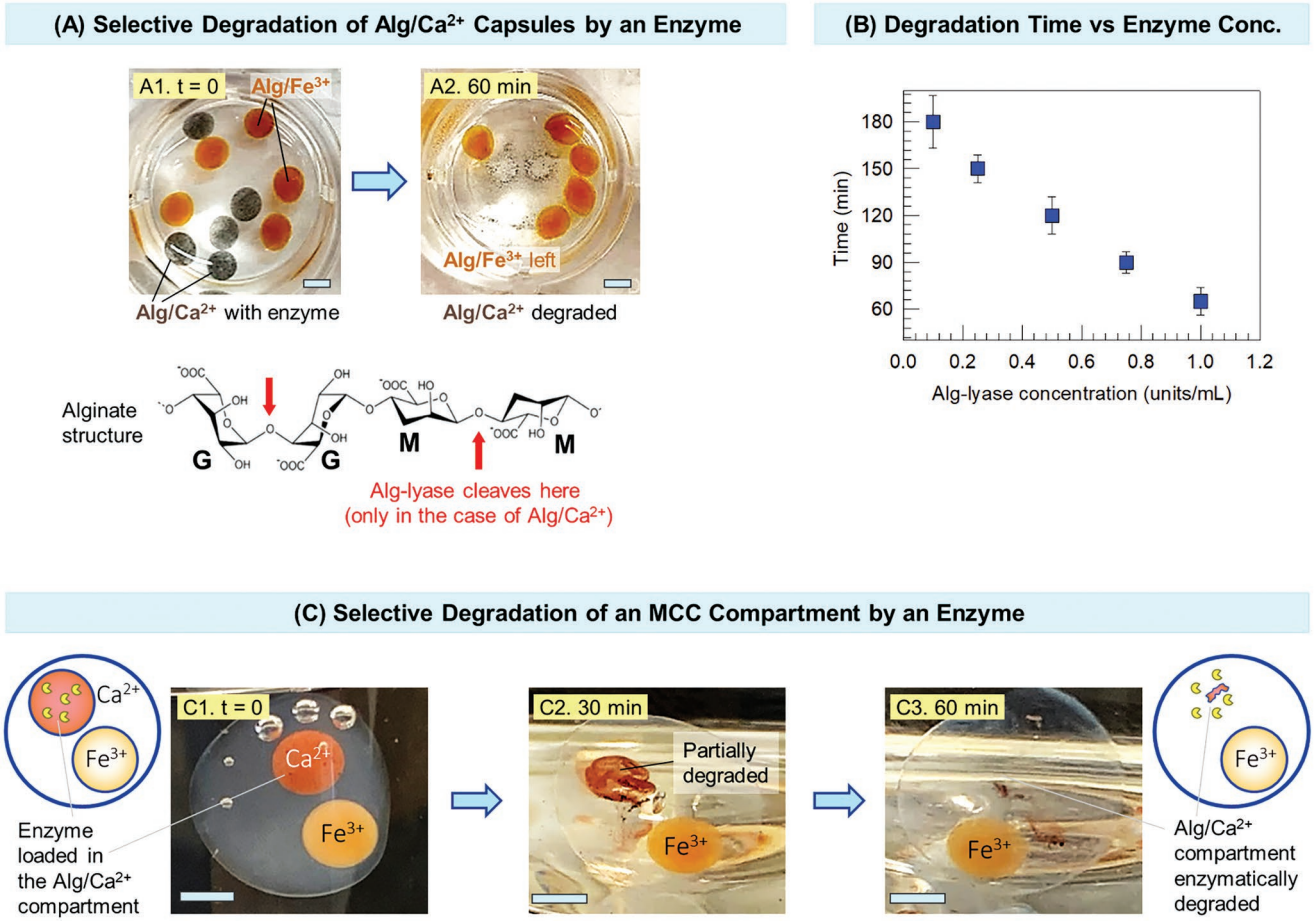

Figure 2. Selective degradation of one compartment in an MCC by the Alg-lyase enzyme. A) The enzyme (1 unit mL^{-1}) degrades Alg/Ca^{2+} capsules (gray) but not Alg/Fe^{3+} capsules (orange). It does so by cleaving Alg chains at the bonds shown by the red arrows. B) Time to completely degrade Alg/Ca^{2+} capsules as a function of the enzyme concentration. Error bars are standard deviations from $n = 5$ measurements. C) Schematic and photos of an MCC with an Alg/Ca^{2+} compartment (red) containing 1 unit mL^{-1} of the enzyme and an Alg/Fe^{3+} compartment (light orange). Only the former is degraded over the course of 60 min. Scale bars: 1 mm.

found that the onset of this selective enzymatic degradation can be triggered by a change in pH. That is, if the MCC is stored in acidic conditions, such as in a sodium acetate buffer (pH 5.2), no degradation occurs for up to four days because Alg-lyase has very low activity at pH 5.2.[16] When the MCC is transferred to PBS (pH 7.4), this serves as an "on" switch to start the enzymatic degradation of the Alg/Ca^{2+} compartment.

2.2. Degradation of a Compartment by H_2O_2

In the previous example, the enzyme selectively degraded the Alg/Ca^{2+} compartment while the Alg/Fe^{3+} one was spared. Next, we present the reverse scenario, which is caused by reactive oxygen species (ROS) generated from H_2O_2. This result is again first shown in a Petri dish containing a suspension of Alg/Fe^{3+} capsules (yellow) and Alg/Ca^{2+} capsules (gray) in acetate buffer (pH 5.2). When 0.1 mM of H_2O_2 is added, only the Alg/Fe^{3+} capsules degrade over the course of 40 min (**Figure 3**A). This degradation occurs because Fe^{3+} reacts with H_2O_2 via Fenton-like reactions (see box in Figure 3A).[22,23] The reactions generate ROS ($HO^{\bullet}$ and $HOO^{\bullet}$), which chemically degrade Alg chains.[24,25] Note that Fe^{3+} is a catalyst for this ROS generation—it is not consumed by the reactions, but instead it shuttles between the ferric (Fe^{3+}) and ferrous (Fe^{2+}) forms via the steps in Figure 3A. Such generation of ROS from H_2O_2 only occurs at low pH,[22,23] which is why we used an acetate buffer. Like in the enzyme case, the time for capsule degradation can be tuned easily by varying the H_2O_2 concentration: Figure 3B shows this time to decrease from 120 min for 88 µmM H_2O_2 to 5 min for 1 mM H_2O_2.

Next, in Figure 3C, we demonstrate selective degradation of an MCC compartment by H_2O_2 in a similar vein to Figure 2C. At $t = 0$, the MCC is placed in acetate buffer and 0.3×10^{-3} mM H_2O_2 is added (Image C1). Within 30 min, the yellow Alg/Fe^{3+} compartment is broken (Image C2) and this degradation is complete in 60 min (Image C3). On the other hand, the Alg/Ca^{2+} compartment (gray) remains intact. Note that the bubbles in the images are oxygen (O_2) gas generated by the H_2O_2 decomposition. The onset of this selective degradation can also be triggered. That is, if the MCC is stored at neutral pH, such as in PBS, no degradation occurs because the H_2O_2

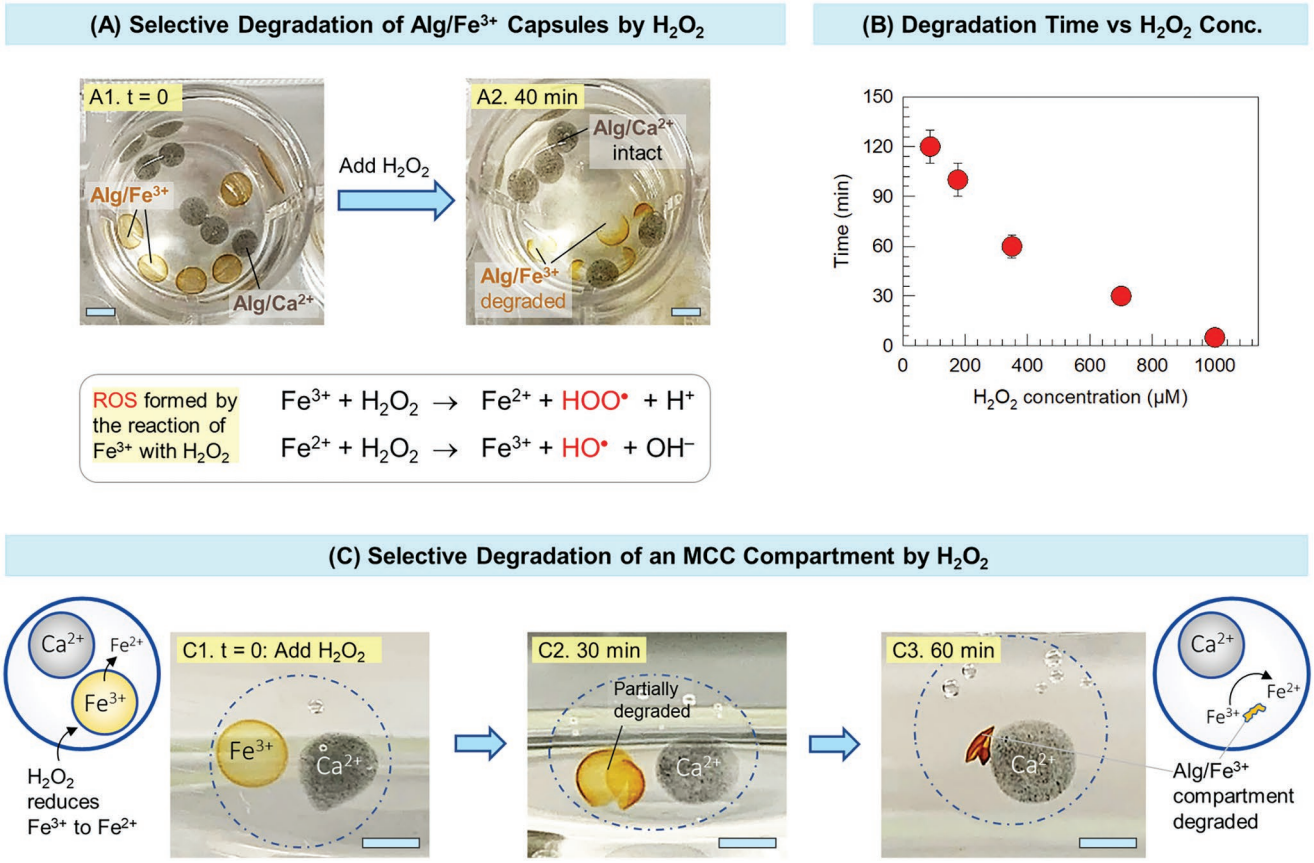

Figure 3. Selective degradation of one compartment in an MCC by H_2O_2. A) H_2O_2 (0.1 mM) degrades Alg/Fe^{3+} capsules (yellow) but not Alg/Ca^{2+} capsules (gray). This is because Fe^{3+} catalyzes the conversion of H_2O_2 to generate ROS (red species in the box) which degrade Alg chains. B) Time to completely degrade Alg/Fe^{3+} capsules as a function of the H_2O_2 concentration. Error bars are standard deviations from $n = 5$ measurements. C) Schematic and photos of an MCC with an Alg/Ca^{2+} compartment (gray) and an Alg/Fe^{3+} compartment (yellow). Upon the addition of 0.3 mM H_2O_2 only the latter is degraded over the course of 60 min. Scale bars: 1 mm.

converts into ROS only at low pH. When acetate buffer is added, it serves an "on" switch for H_2O_2 to start degrading the Alg/Fe^{3+} compartment. Degradations by the Alg-lyase enzyme and H_2O_2 are thus complementary: the former is switched on under neutral conditions, while the latter is switched on under acidic conditions.

2.3. Degradation of a Compartment by UV Light

Fe^{3+} ions complexed to Alg can also be reduced to Fe^{2+} by UV light.[25–27] The light sensitivity is enhanced by adding an α-hydroxy carboxylate like sodium lactate (SLac).[26] Adding SLac causes Fe^{3+} cations to bind both to the carboxylates (COO^-) on SLac as well as those on Alg (**Figure 4**A). The resulting "bidentate ligand" is able to absorb UV light, whereupon an electron from one of the COO^- groups is transferred to the Fe^{3+} ion.[26,28] The net result is that Fe^{3+} gets reduced to Fe^{2+}, as shown by the scheme in Figure 4A. While Fe^{3+} binds strongly to Alg and is therefore an effective cross-linker of Alg chains, Fe^{2+} has only a weak affinity for Alg. Thus, reduction of Fe^{3+} to Fe^{2+} causes the latter to unbind from Alg, thereby removing crosslinks from the capsule and inducing degradation.[25,26] Similar reduction does not occur in the case of Ca^{2+}, and therefore only Alg/Fe^{3+} capsules, but not Alg/Ca^{2+} capsules, should be degradable by UV light.

We thus explored light as another stimulus for compartment degradation. For the experiment in Figure 4A, we took a suspension of Alg/Ca^{2+} capsules (gray) and Alg/Fe^{3+} capsules (orange) in acetate buffer containing 10 mM SLac and exposed the suspension to UV light (365 nm). As expected, only the Alg/Fe^{3+} capsules degrade over 30 min due to the light-induced reduction of Fe^{3+} to Fe^{2+}. The time for UV degradation is dictated by the SLac concentration (Figure 4B), and it decreases from 150 min for 1 mM SLac to 5 min for 50 mM SLac. Figure 4C shows selective degradation of an MCC compartment by UV light. An MCC in acetate buffer with 20 mM SLac is exposed to UV light at $t = 0$ (Image C1). The yellow Alg/Fe^{3+} compartment is partially degraded in 15 min (Image C2) and fully degraded in 30 min. The red Alg/Ca^{2+} compartment remains intact.

2.4. Degradation of a Compartment by a Cascade Process

Next, we demonstrate a cascade process in an MCC, which ultimately causes the selective degradation of one

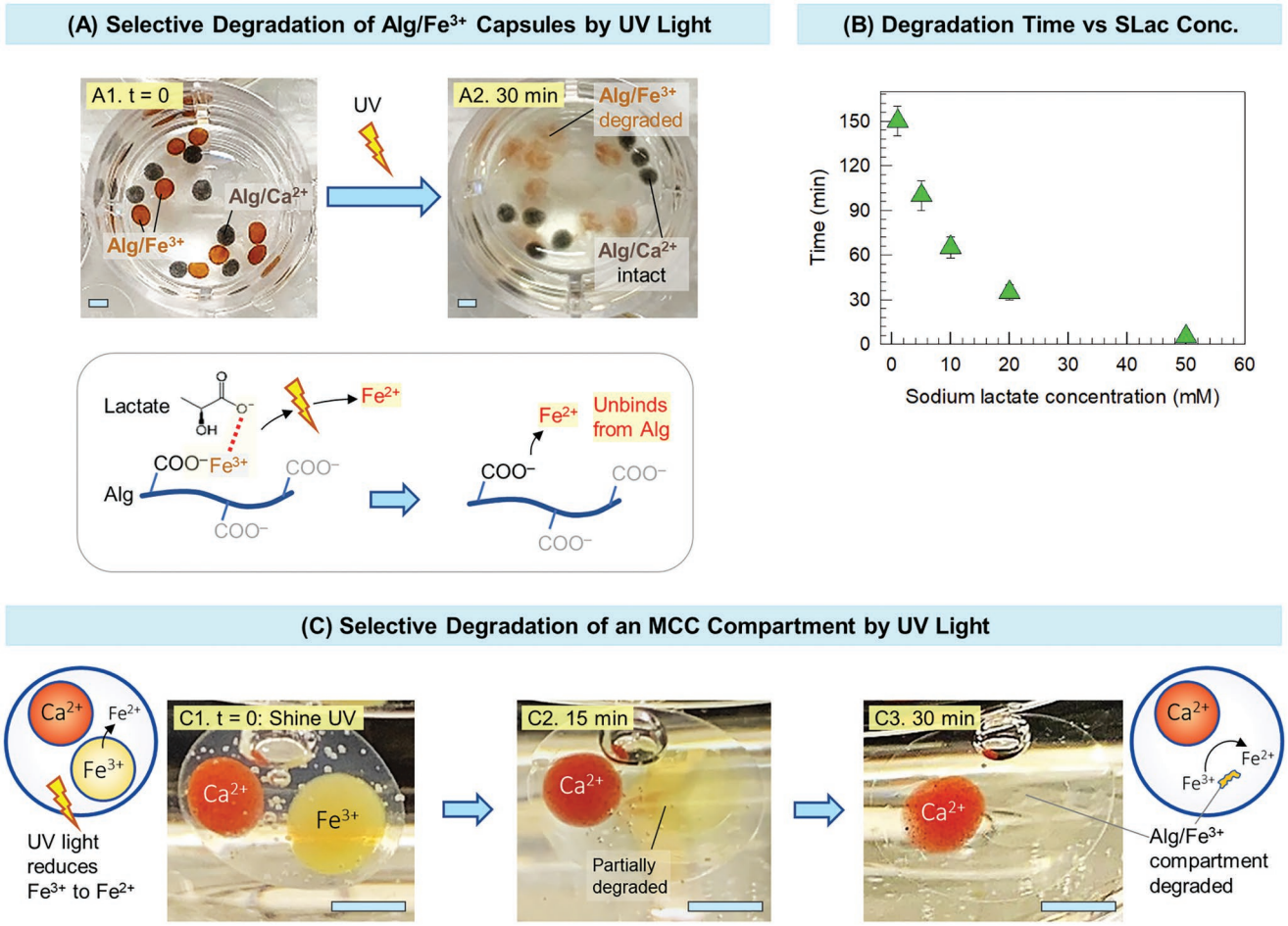

Figure 4. Selective degradation of one compartment in an MCC by UV light. A) In the presence of 10 mM sodium lactate (SLac), UV irradiation degrades Alg/Fe^{3+} capsules (orange) but not Alg/Ca^{2+} capsules (gray). This is because Fe^{3+} is photoreduced to Fe^{2+} by the scheme shown in the box (Fe^{2+} has only a weak affinity for Alg). B) Time to completely degrade Alg/Fe^{3+} capsules as a function of the SLac concentration. Error bars are standard deviations from $n = 5$ measurements. C) Schematic and photos of an MCC with an Alg/Ca^{2+} compartment (red) and an Alg/Fe^{3+} compartment (yellow). In the presence of 20 mM SLac, UV light degrades only the latter over the course of 30 min. Scale bars: 1 mm.

compartment. The cascade employs an enzyme and its reaction product in sequence to induce the degradation (**Figure 5**). The enzyme is glucose oxidase (GOx), which catalyzes the oxidation of glucose, giving H_2O_2 as a by-product. This H_2O_2 is then used to degrade an Alg/Fe^{3+} compartment. Cascade processes inside multicompartment capsules using GOx and glucose have been reported previously, but not to degrade a compartment.[1–5] Figure 5A presents the design of our MCC and it has an Alg/Fe^{3+} compartment (orange) and an Alg/Ca^{2+} compartment (gray) that contains 100 units mL^{-1} of GOx. At $t = 0$, 1% glucose is added to the PBS solution surrounding the MCC. The glucose diffuses into the Alg/Ca^{2+} compartment where it is catalyzed by GOx to produce H_2O_2. The H_2O_2 cascades down to the Alg/Fe^{3+} compartment (Figure 5B), where it reduces Fe^{3+} to Fe^{2+} and hence the compartment degrades over the course of 60 min (Figure 5C). Thus, we have successfully achieved the selective degradation of a compartment. Note also that the cascade is triggered by a small molecule (glucose) that on its own has no effect on either of the compartments.

2.5. Degradation of Both Compartments Sequentially

One limitation of the MCCs discussed thus far is that both the inner compartments (i.e., the "organelles") as well as the MCC lumen around them (i.e., the "cytoskeleton") are made of Alg. Typically, the lumen is a gel of Alg/Ca^{2+}. Thus, if the Alg-lyase enzyme is used to degrade a compartment of Alg/Ca^{2+}, it will also eventually degrade the outer matrix and thereby the whole MCC. We wanted to explore a scenario where the *MCC itself would stay intact* even though both the compartments inside it got degraded. For this, we set out to reinforce the MCC by building a nondegradable outer shell around it. We used a procedure developed recently by our lab that can be used to add a shell of covalently crosslinked polymer around any capsule,[29,30] including MCCs.[12] The procedure (see Figure S2, Supporting Information) involves loading an MCC (~2 mm) with a free-radical initiator, then suspending it in a solution of the monomer acrylamide (AAm) for 5 min. This results in a layer of chemically crosslinked AAm gel (~100 µm thick) around the entire MCC (see the Experimental Section for further details).

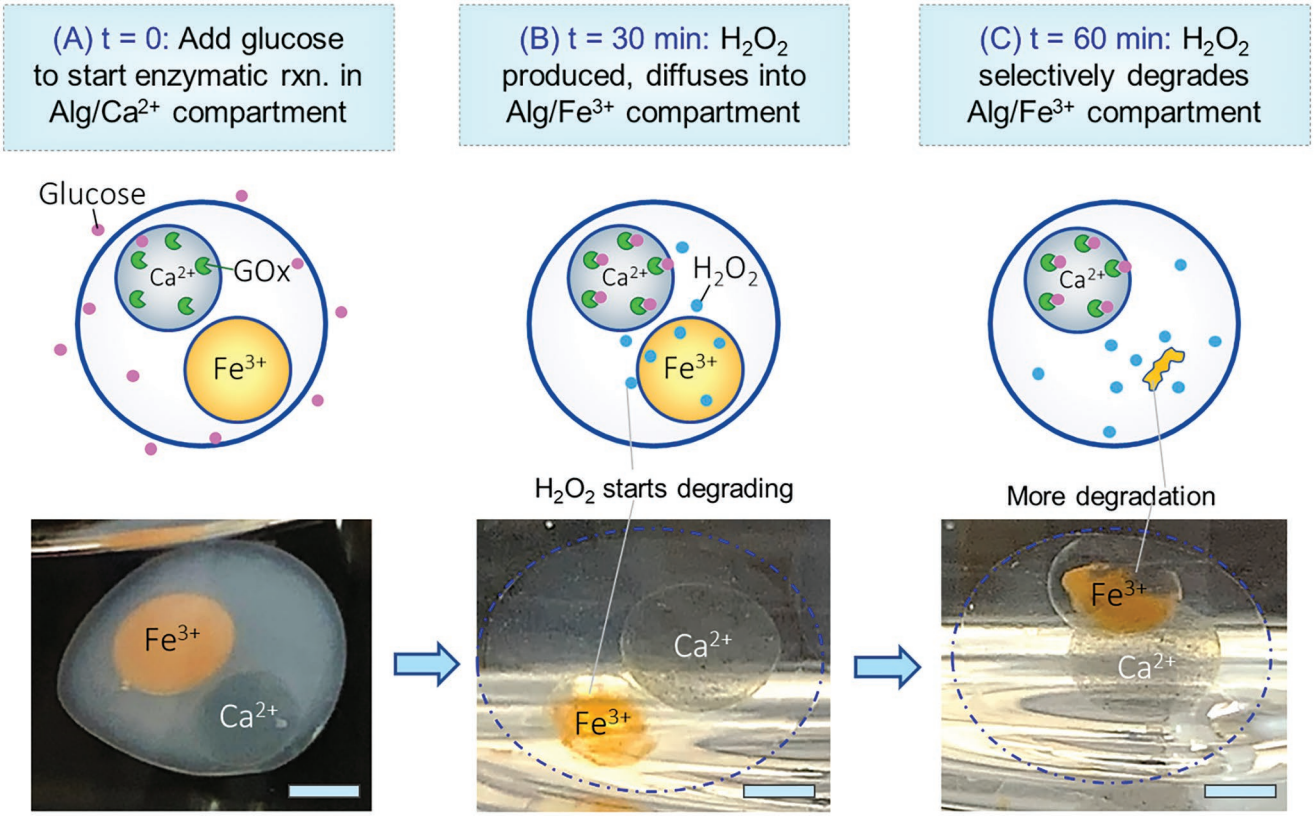

Figure 5. Degradation of a compartment in an MCC by a reaction in an adjacent compartment. The MCC is in PBS and has an Alg/Fe^{3+} compartment (orange) and an Alg/Ca^{2+} compartment (gray) that contains 100 units mL^{-1} of GOx enzyme. A) At $t = 0$, 1% glucose is added to the solution. The glucose is catalyzed by GOx to produce H_2O_2. B) The H_2O_2 diffuses into the adjacent Alg/Fe^{3+} compartment and partially degrades it in 30 min. C) Further degradation of the compartment is seen at the 60 min mark. Scale bars: 1 mm.

We have also shown that this covalent AAm layer is nontoxic to encapsulated species, including both mammalian and microbial cells.

Figure 6A shows an image of the above reinforced MCC in PBS at room temperature. We then added 20 mM SLac to the external solution and exposed the MCC to UV light. Within 30 min, the Alg/Fe^{3+} compartment gets degraded (Figure 6B), as was shown previously in Figure 4. This is again due to the light-induced reduction of Fe^{3+} to Fe^{2+}. We then added 10 units mL^{-1} of Alg-lyase to the external solution, which degraded the Alg/Ca^{2+} compartment over the next 30 min (Figure 6C). Note that the enzyme (~5–10 nm in size) is able to diffuse through the pores in the AAm network (the mesh size of the latter is expected to be ~20 nm). Even after the compartments are degraded, the thin AAm layer around the MCC is still visible (Figure 6D). Because this layer is formed by covalent bonds, it makes the construct robust and allows it to survive the degradation steps.[29,30]

Next, we demonstrate the same sequential degradation of compartments in a reinforced MCC at a smaller (micro) scale. For this, we made the inner compartments of Alg/Fe^{3+} and Alg/Ca^{2+} using the water-air microfluidic device mentioned in the Introduction and discussed in detail in our earlier paper.[11] A schematic of this setup is shown in Figure S3A (Supporting Information) and further details are provided in the Experimental Section. These compartments (~200 µm in diameter) were then encapsulated in microscale MCCs using the same microfluidic setup.[11] In that step, we also introduced the AAm outer layer to reinforce the MCCs, as shown by the scheme in Figure S3C (Supporting Information).[30] In a batch of such MCCs, some have two and others have three inner compartments (**Figure 7**, Panels A1, B1, C1). We included IO-NPs in the Alg/Fe^{3+} compartments to distinguish them in brightfield images. To distinguish the Alg/Ca^{2+} compartments, we included trace amounts of green fluorescent microparticles (GF-MPs) in them. Images from brightfield and fluorescence microscopy are combined using ImageJ for the MCCs shown in Figure 7.

Figure 7A–C presents three sequential degradation schemes (a single MCC is shown in the field of view in each case). First, Figure 7A shows the effect of UV light followed by enzyme. In this case, to the initial MCC (Image A1), 20 mM SLac is added and the sample is exposed to UV light for 30 min—thereby degrading the Alg/Fe^{3+} compartment (Image A2). The remaining Alg/Ca^{2+} compartments are then degraded by adding 10 units mL^{-1} of the Alg-lyase enzyme (Image A3). As the Alg/Ca^{2+} compartments degrade, GF-MPs from these compartments spread throughout the MCC. Figure 7B,C shows how different stimuli used in this study can be mixed and matched to achieve degradation. In Figure 7B, to the initial MCC (Image B1), 1 mM H_2O_2 is added to degrade the Alg/Fe^{3+} compartment (Image B2). Then 10 units mL^{-1} of Alg-lyase is added to degrade

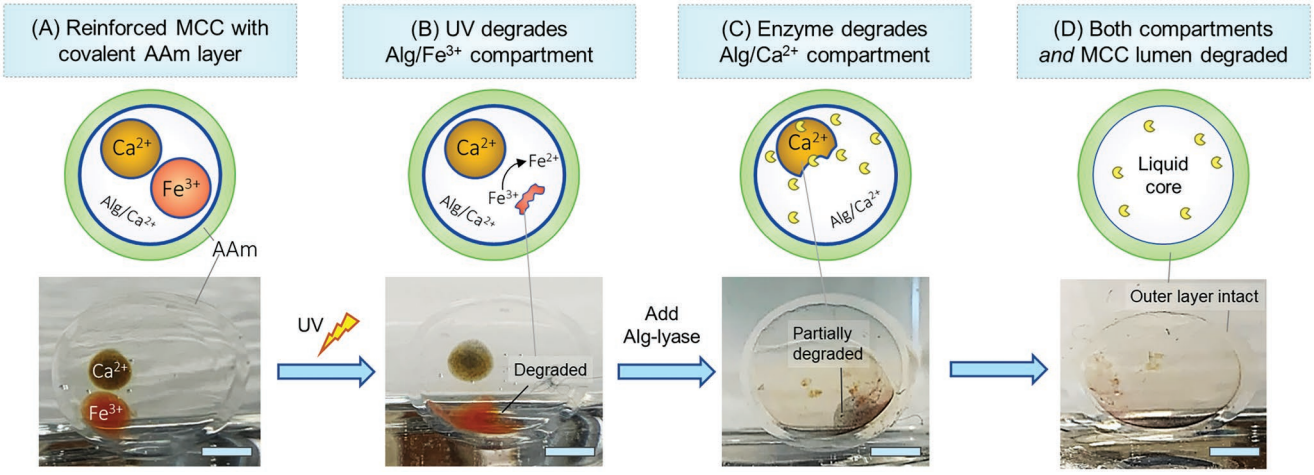

Figure 6. Sequential degradation of both compartments in a reinforced MCC. A) The MCC has an Alg/Fe^{3+} compartment (red) and an Alg/Ca^{2+} compartment (brown). It also has an outer layer of acrylamide (AAm) to reinforce the structure. B) First, the Alg/Fe^{3+} compartment is degraded by adding 20×10^{-3} mM SLac and exposing to UV light for 30 min. C) Next, 10 units mL^{-1} of Alg-lyase is added to degrade the Alg/Ca^{2+} compartment. D) Even after both compartments are degraded, the AAm outer layer remains, keeping the structure intact. Scale bars: 1 mm.

the Alg/Ca^{2+} compartments (Image B3). Finally, in Figure 7C, we change the order of degradation. To the initial MCC (Image C1), 10 units mL^{-1} of Alg-lyase are first added to degrade the Alg/Ca^{2+} compartment (Image C2). After 30 min, 20 mM SLac is added and the sample is exposed to UV light for 30 min to degrade the remaining Alg/Fe^{3+} compartment (Image C3). In all three cases, because of the AAm outer layer, the MCC itself remains intact even after the inner compartments are all degraded.

3. Conclusions

This study demonstrates a platform for making "smart" MCCs with inner compartments that can be selectively degraded by specific stimuli. The MCC platform we had developed earlier was based on the biopolymer Alg: each of the compartments as well as the lumen of the MCC was a gel of Alg. Using the same platform, we achieve smart compartments simply by varying the multivalent cation used to crosslink Alg into a gel. Depending on the cation, the compartments are responsive to stimuli that include biochemical cues (enzymes), chemical cues (ROS), and physical cues (UV light). First, Alg/Ca^{2+} compartments in an MCC are shown to be selectively degraded by Alg-lyase enzymes (the enzyme cleaves Alg chains into oligomers). On the other hand, Alg/Fe^{3+} compartments are selectively degraded by ROS generated from H_2O_2 (the ROS again break Alg chains). Alg/Fe^{3+} compartments can also be degraded by irradiation with UV light in the presence of a sacrificial carboxylate (the UV reduces Fe^{3+} to Fe^{2+} and the latter unbinds from Alg, thereby removing crosslinks). Selective degradation of compartments is shown with MCCs at two different length scales: macro and micro. Stimuli can be mixed and matched in any order because the responses are orthogonal to each other, i.e., one stimulus affects only one kind of compartment. In cases where all the inner compartments are degraded, the MCC can still remain intact if it is endowed with a covalently crosslinked outer layer. All in all, our study shows the versatility of MCCs based on Alg: we can make MCCs with distinct payloads in each compartment and then designate *which compartment(s)* to degrade, as well as the *order* in which they degrade. The ability to create such smart MCCs is an important step in enabling cell-like architectures to emulate the novel behaviors seen in biology.

4. Experimental Section

Materials: The following chemicals were purchased from Sigma-Aldrich. These included the biopolymers alginate (Alg), which was the sodium salt of a medium viscosity alginic acid extracted from brown algae, and xanthan gum (XG). Materials needed to form the outer layer by free-radical polymerization included the monomer AAm, the crosslinker N,N′-methylene-bis(acrylamide) (BIS), the initiator ammonium persulfate (APS), and the accelerator tetramethylethylene diamine (TEMED). The enzymes used in this study were glucose oxidase (GOx) from *Aspergillus niger* (100 000 units g^{-1}) and alginate lyase (Alg-lyase) (≥10 000 units g^{-1}). Other salts and chemicals used in this study included sodium acetate, calcium chloride dihydrate ($CaCl_2$), ferric chloride ($FeCl_3$), sodium chloride (NaCl), D-glucose, and PBS. Items purchased from other vendors included sodium lactate from Santa Cruz Biotechnology; hydrogen peroxide (H_2O_2, 30% solution in water) from Thermo-Fisher; Fluoresbrite Carboxy YG green-fluorescent microparticles (GF-MPs, 3 µm diameter) from Polysciences; IO-NPs from Lanxess and CB-NPs (N110) from Sid Richardson Carbon Company.

Synthesis of Macroscale Capsules: Alg capsules (with specific payloads) were prepared as follows. First, a feed solution of 2% Alg containing appropriate payloads (such as enzymes) was prepared in deionized (DI) water. This was then dropped into a 0.1 M solution of the appropriate salt ($CaCl_2$ or $FeCl_3$) using a syringe with a 22-gauge needle. The Alg droplets were allowed to incubate in the salt solution typically for 1 h at 4 °C, whereupon the droplets were converted into Alg/Ca^{2+} or Alg/Fe^{3+} capsules with diameters of ≈500 µm. The capsules were washed with DI water and stored in DI water at 4 °C until further use. These capsules served as the inner compartments in the MCCs. For color contrast, trace amounts (~0.01%) of CB-NPs, IO-NPs, or GF-MPs were included in the Alg feed. To create Alg capsules with encapsulated Alg-lyase enzyme, sodium acetate buffer (pH 5.2) was used instead of PBS to make the Alg feed.

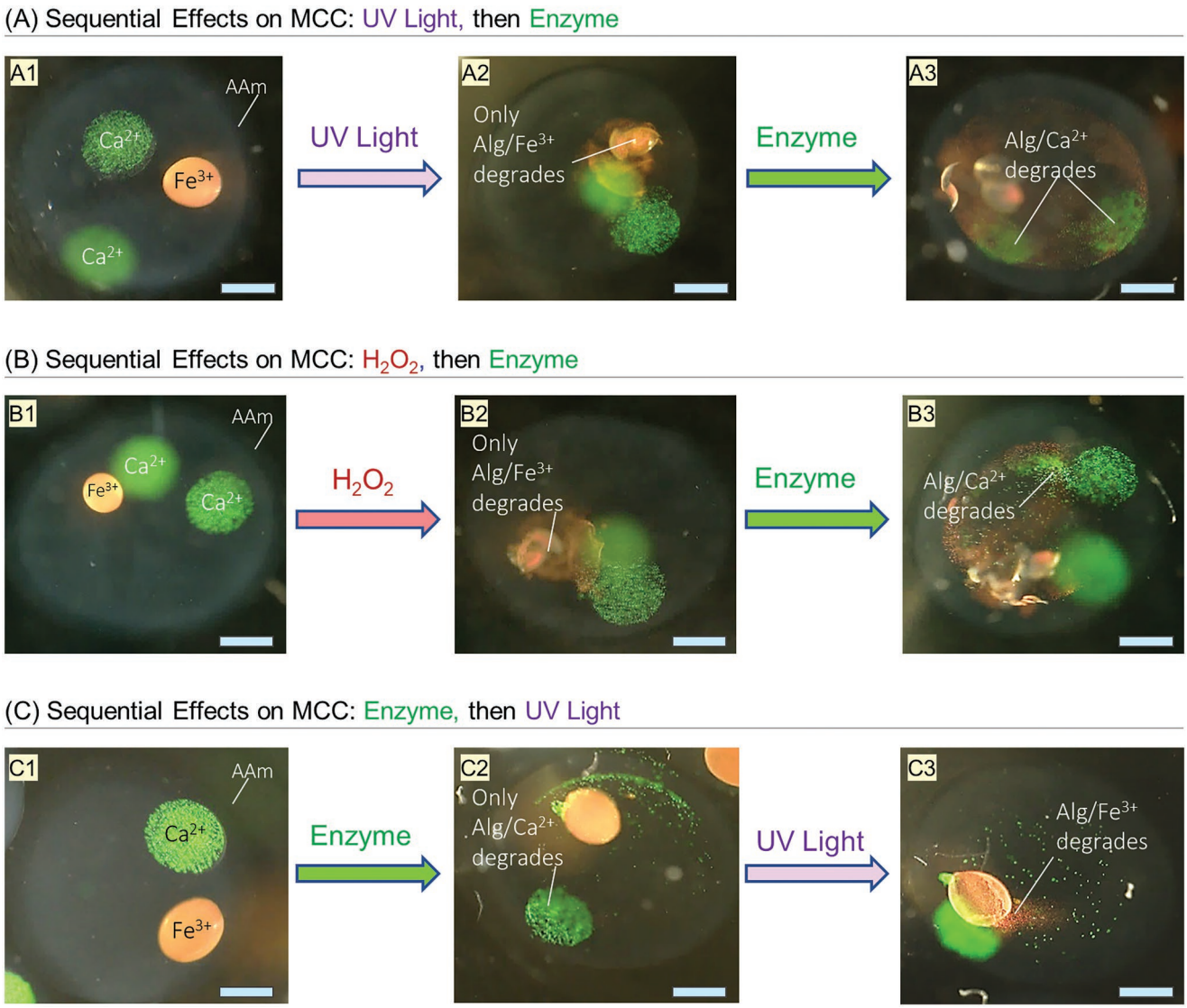

Figure 7. Sequential degradation of both compartments in reinforced microscale MCCs. All images are superpositions of those from brightfield and fluorescence microscopy. The MCCs have two or three compartments as well as an AAm outer layer to reinforce the structures. The Alg/Fe^{3+} compartments are orange while the Alg/Ca^{2+} compartments are green. A) Alg/Fe^{3+} is degraded by UV light and then the Alg/Ca^{2+} by the Alg-lyase enzyme. B) Alg/Fe^{3+} is degraded by ROS from H_2O_2 and then the Alg/Ca^{2+} by the Alg-lyase enzyme. C) Alg/Ca^{2+} is degraded by the Alg-lyase enzyme and then the Alg/Fe^{3+} by UV light. In all cases, each stimulus only degrades a specific type of compartment, indicating that the stimuli are orthogonal to each other. The AAm layer maintains the MCC even when the compartments are all degraded. Scale bars: 200 µm.

Synthesis of Macroscale MCCs: Alg/Ca^{2+} and Alg/Fe^{3+} capsules were mixed in equal ratio in a 2 wt% Alg solution in DI water and this suspension was used as the feed to make MCCs (see schematic in Figure S1, Supporting Information). Using a transfer pipette, droplets from this suspension were introduced into a 0.1 M $CaCl_2$ solution and allowed to incubate for 1 h at 4 °C. This resulted in MCCs (diameters ~5 mm) in which the original capsules were inner compartments. The MCCs were washed with DI water and stored in DI water until further use.

Synthesis of Macroscale MCCs with a Covalent Outer Layer: MCCs from the above step were soaked in a 15 mg mL^{-1} solution of the initiator APS for 2 min. The APS-loaded MCCs were then suspended in a monomer solution made by dissolving 10% AAm, 0.034% cross-linker (BIS), 1.5% accelerant (TEMED), and 1.5% thickener (XG). Polymerizations were conducted at room temperature for 5 min, whereupon a 100-µm-thick AAm layer formed around the MCCs, as shown by the schematic in Figure S2 (Supporting Information). The resulting structures were washed three times with DI water and then stored in DI water.

Synthesis of Microscale Capsules: Microcapsules were prepared using a microfluidic method developed by this group that was described in detail previously and is shown schematically in Figure S3 (Supporting Information).[11] The feed was a 2% Alg solution in DI water while the reservoir was a 0.1 M solution of the appropriate salt ($CaCl_2$ or $FeCl_3$). Using a syringe pump, the feed was flowed through a glass capillary with an inner diameter of 200 µm. Compressed nitrogen gas was sent as a sheath around the capillary. A gas-flow controller was connected to a function generator (BK Precision) to generate gas pulses, with the gas pressure set at 10 psi. For every pulse of gas, an aqueous droplet was dislodged from the tip of the capillary. Droplets entered the unstirred reservoir, where they were converted to microcapsules upon incubation for 5 min. The feed flow rate (typically 40 µL min^{-1}) as well as the frequency of the pulsing gas (typically 1 Hz) dictated the sizes of the

droplets and thereby of the resulting microcapsules.[11] Microcapsules prepared in this study had diameters ~200 µm. They were filtered, washed, and stored in DI water. For color contrast, GF-MPs were included in the feed in making the Alg/Ca^{2+} microcapsules.

Synthesis of Microscale MCCs with a Covalent Outer Layer: The procedure to make microscale capsules with a covalent layer in a single step was described in an earlier paper.[30] Here, it is adapted to the case of MCCs, as shown schematically in Figure S3C (Supporting Information), but with a few changes to the feed and reservoir solutions. The feed was made by combining Alg/Ca^{2+} and Alg/Fe^{3+} microcapsules (~200 µm diameter) in an equal ratio in a solution containing 2% Alg and 1.5% APS. This was flowed by a syringe pump through a capillary with an inner diameter of 500 µm at a flow rate of 40 µL min^{-1}. Pulses of gas (at 1 Hz) were used, as above, to dislodge droplets from the capillary tip, which then entered a reservoir solution of 10% AAm, 0.034% BIS, 1.5% TEMED, and 1.6% $CaCl_2$ in DI water. Within 5 min, MCCs were formed with an AAm outer layer and with the Alg/Ca^{2+} and Alg/Fe^{3+} as inner compartments. The MCCs were filtered, washed, and stored in DI water.

Degradation Experiments: Experiments with multiple Alg/Ca^{2+} and Alg/Fe^{3+} capsules (Figures 2A, 3A, and 4A) were done by suspending identical numbers of these capsules in the appropriate solution in a small Petri dish. The dish was examined at regular intervals to visually assess the extent of degradation over time. In the case of enzymatic degradation, the capsules were suspended in PBS and the Petri dish was kept in a 37 °C incubator. For experiments at different enzyme or H_2O_2 or SLac concentrations (Figures 2B, 3B, and 4B), the appropriate capsules were placed in different wells of a 24-well Petri dish. Different concentrations of enzyme were added to the wells and the Petri dish was transferred to a 37 °C incubator. The system was then monitored over time. Degradation by H_2O_2 was studied at room temperature for capsules in sodium acetate buffer (pH 5.2). Degradation by UV light was studied at room temperature for capsules in normal saline containing SLac. Samples were irradiated with light at 365 nm from a Mineralight lamp (Model UVGL-58). For degradation experiments with MCCs (Figures 2C, 3C, and 4C), the MCC was suspended in 5 mL of the appropriate solution in a small vial. The same procedures as above were followed for degradation by each of the stimuli.

Capsule Degradation in a Cascade Process: MCCs were synthesized as described above with an Alg/Ca^{2+} compartment loaded with 100 units mL^{-1} of GOx enzyme and an Alg/Fe^{3+} compartment. This MCC was then suspended in 5 mL of PBS containing 1 wt% of D-glucose and the experiment (Figure 5) was carried out at room temperature.

Sequential Degradation of MCC Inner Compartments: MCCs with an AAm outer layer were used in the sequential degradation studies (Figures 6 and 7). In the case of UV followed by enzymatic degradation, the MCC was first placed in 5 mL of normal saline to which 20 mM of SLac was added. The sample was exposed to UV light (365 nm) for 30 min, which degraded the Alg/Fe^{3+} compartment in the MCC. Next, the same MCC was transferred to PBS and 10 units mL^{-1} of Alg-lyase was added to trigger degradation of the Alg/Ca^{2+} compartment. Similar steps were done for the other sequences of stimuli discussed in Figure 7.

Optical Microscopy: Images under brightfield and fluorescence of the microscale MCCs were obtained using an Olympus MVX10 microscope. The images were overlaid using the ImageJ software.

Statistics: Values of the degradation time shown in Figures 2–4 were measured and used without any transformation or normalization. At least five samples were tested for each data point. No outliers were excluded. Mean values are shown in the plots, and error bars correspond to standard deviations. Statistics were calculated and plotted using Excel and SigmaPlot.

Supporting Information

Supporting Information is available from the Wiley Online Library or from the author.

Acknowledgements

This study was partially funded by NSF CBET #1844299 and the Army Research Laboratory (ARL) and the Army Research Office (ARO) under Grant No. W911NF-18-2-0170.

Conflict of Interest

The authors declare no conflict of interest.

Data Availability Statement

The data that support the findings of this study are available from the corresponding author upon reasonable request.

Keywords

adaptive materials, artificial cells, cell mimics, degradable capsules, degradable gels, protocells, responsive materials

Received: October 30, 2022
Revised: February 5, 2023
Published online: March 9, 2023

[1] M. Marguet, C. Bonduelle, S. Lecommandoux, *Chem. Soc. Rev.* **2013**, *42*, 512.
[2] C. Xu, S. Hu, X. Y. Chen, *Mater. Today* **2016**, *19*, 516.
[3] M. J. York-Duran, M. Godoy-Gallardo, C. Labay, A. J. Urquhart, T. L. Andresen, L. Hosta-Rigau, *Colloids Surf., B* **2017**, *152*, 199.
[4] B. C. Buddingh, J. C. M. van Hest, *Acc. Chem. Res.* **2017**, *50*, 769.
[5] X. M. Qian, I. N. Westensee, E. Brodszkij, B. Stadler, *Wiley Interdiscip. Rev. Nanomed. Nanobiotechnol.* **2021**, *13*, e1683.
[6] B. Alberts, *Molecular Biology of the Cell*, Garland Publishers, New York, **2002**.
[7] P. L. Luisi, *The Emergence of Life: From Chemical Origins to Synthetic Biology*, Cambridge University Press, Cambridge, UK **2006**.
[8] A. H. Chen, P. A. Silver, *Trends Cell Biol.* **2012**, *22*, 662.
[9] N. A. Yewdall, A. F. Mason, J. C. M. van Hest, *Interface Focus* **2018**, *8*, 20180023.
[10] V. I. Titorenko, R. A. Rachubinski, *Nat. Rev. Mol. Cell Biol.* **2001**, *2*, 357.
[11] A. X. Lu, H. Oh, J. L. Terrell, W. E. Bentley, S. R. Raghavan, *Chem. Sci.* **2017**, *8*, 6893.
[12] K. C. DeMella, S. N. Subraveti, K. J. Perry, S. P. Karna, S. R. Raghavan, *Adv. Funct. Mater.* **2022**, *32*, 2110191.
[13] N.-N. Deng, M. Yelleswarapu, W. T. S. Huck, *J. Am. Chem. Soc.* **2016**, *138*, 7584.
[14] X. M. Liu, P. Zhou, Y. D. Huang, M. Li, X. Huang, S. Mann, *Angew. Chem., Int. Ed.* **2016**, *55*, 7095.
[15] C. L. Mou, W. Wang, Z. L. Li, X. J. Ju, R. Xie, N. N. Deng, J. Wei, Z. Liu, L. Y. Chu, *Adv. Sci.* **2018**, *5*, 1700960.
[16] R. S. Ashton, A. Banerjee, S. Punyani, D. V. Schaffer, R. S. Kane, *Biomaterials* **2007**, *28*, 5518.
[17] S. K. Leslie, D. J. Cohen, J. Sedlaczek, E. J. Pinsker, B. D. Boyan, Z. Schwartz, *Biomaterials* **2013**, *34*, 8172.
[18] Y. Zhu, L. Wu, Y. Chen, H. Ni, A. Xiao, H. Cai, *Microbiol. Res.* **2016**, *182*, 49.
[19] G. Huang, Q. Wang, M. Lu, C. Xu, F. Li, R. Zhang, W. Liao, S. Huang, *Mar. Drugs* **2018**, *16*, 120.

[20] M. B. Dowling, A. S. Bagal, S. R. Raghavan, *Langmuir* **2013**, *29*, 7993.
[21] A. Gupta, J. L. Terrell, R. Fernandes, M. B. Dowling, G. F. Payne, S. R. Raghavan, W. E. Bentley, *Biotechnol. Bioeng.* **2013**, *110*, 552.
[22] W. G. Barb, J. H. Baxendale, P. George, K. R. Hargrave, *Nature* **1949**, *163*, 692.
[23] J. De Laat, H. Gallard, *Environ. Sci. Technol.* **1999**, *33*, 2726.
[24] M. Gamella, M. Privman, S. Bakshi, A. Melman, E. Katz, *ChemPhysChem* **2017**, *18*, 1811.
[25] D. M. Roquero, A. Othman, A. Melman, E. Katz, *Mater. Adv.* **2022**, *3*, 1849.
[26] R. P. Narayanan, G. Melman, N. J. Letourneau, N. L. Mendelson, A. Melman, *Biomacromolecules* **2012**, *13*, 2465.
[27] G. E. Giammanco, C. T. Sosnofsky, A. D. Ostrowski, *ACS Appl. Mater. Interfaces* **2015**, *7*, 3068.
[28] J. Chen, W. R. Browne, *Coord. Chem. Rev.* **2018**, *374*, 15.
[29] B. C. Zarket, S. R. Raghavan, *Nat. Commun.* **2017**, *8*, 193.
[30] S. H. Ahn, M. Rath, C. Y. Tsao, W. E. Bentley, S. R. Raghavan, *ACS Appl. Mater. Interfaces* **2021**, *13*, 18432.